

Hardware Design for Optical Tomography Sensor Configuration Using Two Orthogonal and Two Rectilinear Projections Arrays

Ruzairi Abdul Rahim¹, Pang Jon Fea¹, Chan Kok San¹

¹ Faculty of Electrical Engineering, Universiti Teknologi Malaysia, 81310 UTM Skudai, Johor, Malaysia

Corresponding author* email: ruzairi@utm.my

Available online 30 December 2023

ABSTRACT

This paper represents the configuration of optical tomography sensor by using infrared emitter and phototransistor. The projection geometry of the sensor is based on the combination of two orthogonal and two rectilinear projections arrays. A fixture is designed for holding all emitter-receiver pairs in parallel. Selection of phototransistor is explained so that the tomography sensor developed is free of noise cause by surrounding environment. This paper describes all points to be considered when design an optical tomography sensor.

Keywords: optical tomography, infrared emitter

1. INTRODUCTION TO PROCESS TOMOGRAPHY

The development of process tomography started in the medical field for non-intrusive investigation of living animals. Most people today associate tomography with complex systems used to obtain images on internal parts of the human body. Tomography system, however, have applications in other areas of science and technology. Some of the medical techniques are used in process industries. However, special methods have been developed for process industries. For example, a project on electrical capacitance tomography for imaging multiphase flow from oil wells and in pneumatic conveyors began at University of Manchester Institute of Science and Technology in England (UMIST) [1].

Process tomography evolved in the late 1980's to meet a widespread need for the direct analysis of the internal characteristic of process plants in process instrumentation to utilize resources more efficiently, and to satisfy demand and legislation for product quality and to reduce environment emissions. The measuring instruments for such applications must use robust, non-invasive sensors which, if required, can operate in aggressive and fast moving fluids and multiphase mixtures. A potentially good solution for many of these types of problem is to use process tomography. The tomographic imaging of objects offers a unique opportunity to unravel the complexities of the structure without the need to invade the object.

Flow imaging is an example of the general area known as process tomography. The changing properties of the flow at a particular time can be visualized on a computer screen. This system could be extended to analyze the image data and define a flow in term of flow regime.

The specific characteristic of tomographic measurement is its proven ability to interrogate the dynamic state of process condition within a unit operation such as a mixing vessel or conveyor without interfering with the process itself. This is achieved by using non-invasive sensors along a cross sectional boundary of the process equipment. The tomographic measurement data is manipulated using algorithms for image reconstruction, profile analysis and computation of numerical quantities such as flow rates, concentration, size and phase distribution. From the knowledge of material distribution and movement, improved internal models involving kinetic and dynamic parameters can be derived and used as an aid to optimize process design.

By successfully developing different types of tomography techniques, application of tomography in industrial sectors is increasing everyday. Those industrial fields include bulk chemicals, food processing, minerals processing, pharmaceuticals, polymers and plastics, pulp and paper and oil and gas [2]. Basically, process tomography can be applied in many types of processes and unit operations, including pipelines, stirred reactors, fluidizer beds, mixers and separator. Normally, the tomography system being used consists of three components that are sensor, the data acquisition system and the data manipulating system together with the display unit. Sensors are usually positioned around the inner part of the vessel or pipe to be imaged. The number of sensors used will provide the resolution of the detection region and accuracy of the profile to be measured. The sensor output signal depends on the position of the component boundaries

within their sensing zones. A computer is used to reconstruct the tomographic image of the cross section being observed by the sensors. The common tomography system in industry process with their applications is presented in Figure 1.

In Figure 1, we notice that there are a lot of sensor types which can be used in process tomography. Different sensor works with different method to produce the output signal, which might have advantages and disadvantages over the others depending on the structure of the sensors. The usage of a suitable sensor in a certain process depends on the physical characteristics of the conveying system and the requirement of the parameter to measure and presented.

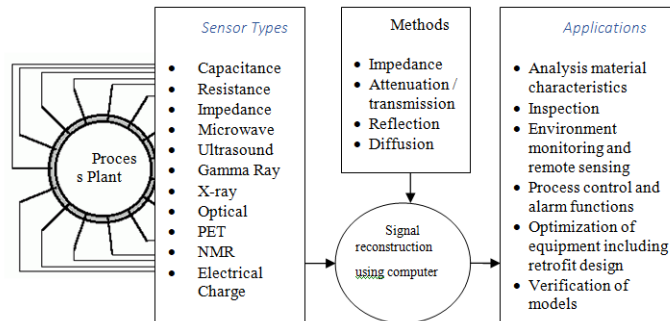


Figure 1: Sensor types, methods and applications for process tomography

Process tomography involves the acquisition of measurement signals from sensors located at the periphery of an object [3]. The parameter or characteristic to be imaged is determined by the type of sensor chosen, such as gamma-rays and X-rays are sensitive to density, while capacitance sensors are sensitive to the dielectric constant of the object. To construct cross-sectional image, the sensor signals are amplified, filtered, digitized and finally be processed in a computer using certain image reconstruction algorithm. Normally, most of the flow information is based on the cross-sectional image. For example, the cross-sectional image itself already provides flow material's concentration. On the other hand, hundreds set of upstream and downstream images can provide flow velocity when correlation function is applied in this case. As a result, process tomography will provide an increase in the quantity and quality of information when compared to many earlier measurement techniques [4].

2. OVERVIEW OF OPTICAL TOMOGRAPHY SENSOR

The optical sensors based on radiation-attenuation technique is one of the 'hard-field' sensors which is similar to gamma ray tomography in which the sensing field is based on the measurement of the attenuation or absorption of radiation. Optical sensor allows the use of very effective and accurate reconstruction algorithm developed for medical X-ray CT [5]. The advantages of optical sensors are the speed of light makes the response time negligible, the small wavelength can potentially provide very high resolution, measurements are immune to electrical noise or interference and the wide selection of readily available emitters and detectors [6].

The utilization of optical sensors using visible light and infrared in a process tomography system is not a latter invention but the progression is weak compared to electrical capacitance tomography due to the penetration factor of the light sources. Several research have been carried out to develop an optical tomography system for different applications. The research include measurement of bubble in conveying fluid by Xie [7], Dugdale [8], Ibrahim [9] and Rzasa[10], flow imaging and measurement in pneumatic conveyor by Abdul Rahim [4] and Chan [11], combustion process monitoring in engine by Lucas [12] and sewage system monitoring by Daniels [13].

The principle used in optical tomography involves projecting a beam of light through a medium from one boundary point and detecting the level of light received at another boundary point [4]. The optical tomography system can be designed using a group of emitter-receiver pairs such as light emitting diode (LED) and photo detector [14]. Besides, the light transmitter mediums such as fiber optic can be used to increase the number of sensors being used. Usually, several groups of transmitter and receiver pairs are used in a system to provide better solution and to minimize the aliasing that occurs when two particles intercept the same view.

The analogue voltage signals produced by photo detectors show the amount of attenuation in the path of the beam caused by the flow regime. The proper use of electronic circuit is able to measure at least two physical parameters of the flowing object in conveyor. The first measurement is the intensity of received light that is related to the distribution of flowing object, while the other measurement is differential of light signal that is related to particle flow rate [11].

Optical tomography involves the use of non-invasive optical sensors to obtain vital information in order to produce images of the dynamic internal characteristics of process system [9]. It has the advantages of being conceptually straightforward and relatively inexpensive. The optical tomography system uses a number of light emitter-receiver pairs and a wide variety of light sources such as visible light, infrared or laser light.

A general optical tomography system requires a sensor fixture, a number of optical sensor arrays, signal measurement circuitry, data acquisition system and a computer as data processing unit and display unit. Its working principle involves projecting a beam of light through a medium from one boundary point and detecting the level of light received at another boundary point [4]. For the type of projection used in the system, it can be parallel beam (orthogonal) projection, rectilinear projection, fan beam projection or mix projection among them.

Optical tomography has the application of pneumatic conveying in the industry of food processing, plastic product manufacturing and solids waste treatment. The specific measurements of it are flow concentration, flow velocity and mass flow rate determination. Besides, optical tomography sensor also can measure gas bubbles and particles in conveying fluid.

2.1 Types of Projections

A single transducer pair termed a 'view' basically consists of transmitter and receiver. The transmitter is able to transmit a specific source through a specific medium and the transmitted signal is able to retrieve by the corresponding receiver. The retrieved signal provided specific information such as density, permittivity, attenuation coefficient etc. A single view holds a very little information about the material flow in a conveyer since it only covers a small region of the sensing area. Thus, to get a coverage information profile, several views are required. With the combination of several into a group, a 'projection' is formed. The projection measurement will provide more significant information of the flow regimes across the vessel than the single view.

Various forms of projection have been developed for different types of sensors. Generally, there are four types of main projections for tomography. They are the parallel projection, fan beam projection, ultrasonic echo projection and electrostatic field projection. Figure 2 shows main projections type for tomography.

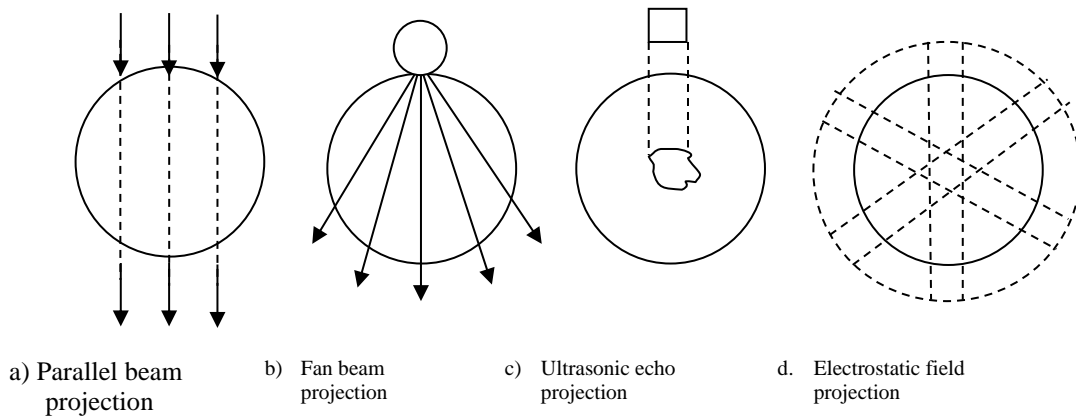


Figure 2. Various form of projections through a cross-section of conveyor, pipe-line or vessel

Parallel projection (Figure 2a) is always used in radiation methods, such as X-rays, gamma rays and light. Basically, one set of parallel projection cannot pinpoint the exact position of the flowing particles but this can be solved by using placement of another set of projection in different axes.

Figure 2b shows a fan beam projection method. This method uses a single projection from radiation source and associates with a number of detectors from different angle. An alternative to the arrangement is a technique in which single photon-energy measuring detector and multi-channel analyzer is used with a number of radiation sources that have different energy.

Ultrasonic echo projection (Figure 2c) is a method normally used with ultrasonic sensor in which the same sensor can be used for transmitting and receiving information of the presence and the distance of the flowing material. To get a better resolution image, the multiple beams concept is applied in sequence, such arrangement is commonly used in clinical where the transducer is rotated about an arc by a small motor. This improvement is called B scan. Figure 2d shows another kind of projection using electrostatic field sensing zones produced by capacitance plate sensor distributed around the surface of the pipe.

3 HARDWARE DESIGN

In optical tomography system, the two types of sensor arrangement techniques that have been investigated and applied to measure gas/solid flows are parallel beam projection and fan beam projection. For parallel beam projection, the number of emitter and receiver are the same. Each pair of transmitter-receiver is arranged in a straight line and the received signal only corresponds to its emitter source. While for fan beam projection, the number of emitters and receivers can be unequal. A multiplexing source is used and all the receivers produce the signals corresponding to each multiplexed source. The fan beam projection technique provides a higher resolution system compared to the same number of sensors used in parallel projection due to high obtaining information [16]. However, it has the weakness like hard to model the sensitivity map of each sensor projection in forward problem and a longer time to reconstruct the cross-sectional image compared to parallel beam projection technique.

A typical optical tomography system consists of a sensor, an electronic circuit, a data acquisition system, and a host computer as data processing and display unit. For the developed system, the block diagram of Figure 3 is applied.

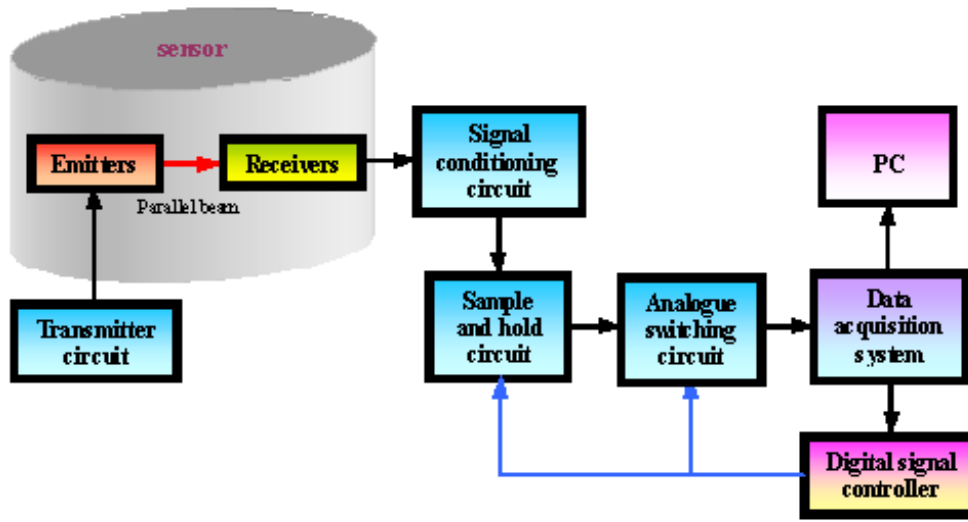


Figure 3. Block diagram of developed system

A transmitter circuit will switch on the emitters' light and project them to receivers. The signal conditioning circuit now converts the signals received into voltage readings and then amplifies them to a sufficient level. Finally, the output signals pass through sample and hold circuit to the analogue switching circuit and the data acquisition system based on the control signals from digital signal controller. Next, data acquisition system will digitise the signals and flow them into computer for further processing.

3.1 Selection of emitter and receiver

The previous research by [16] successfully applied the LED as the emitter in optical tomography system. However, the light of LED is visible light with the wavelength in between 380-700 nm and therefore results in the tomography sensor designed is easily getting noise from the surrounding environment light source. It must be noted that most of the light sources such as incandescent lamp and fluorescent light (peak of radiant power at 550 nm) are widely used in the indoor factory. Unless there are solutions to prevent the surrounding light from projecting into tomography sensor, it is not suitable to be used in most of the indoor factories.

By referring to Figure 4, the wavelength of infrared is in between 700 – 1000nm. It is far away from the wavelength of fluorescent light and this is the reason that infrared emitter is used in this project. The infrared emitter model, TSUS4300 from TEMIC Semiconductor is chosen because of some main reasons, such as its physical size with 3 mm in diameter, wavelength in the range of 900 to 1000 nm, peak of wavelength at 950 nm, small angle of half intensity which is 16 degree and can be easily acquired from the local market.

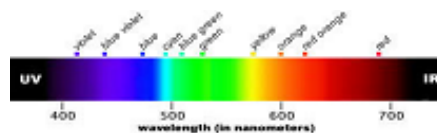


Figure 4. Wavelength of light

Regarding to the photo-detector selection, the photodiode and phototransistor were being considered because their physical sizes are small, wavelength covering infrared light and also inexpensive. However, the final selection is the phototransistor based on two factors. First, the phototransistor model, TEFT4300 is specifically manufactured for the IR emitter TSUS4300. Second, based on the graph of spectral sensitivity versus wavelength in the corresponding datasheet, the starting wavelength of phototransistor TEFT4300 is about 875 nm, which is quite a distance away from the visible light's boundary, 700nm. But, most of the photodiodes have the starting value from the visible light's wavelength. Besides, its physical size with 3 mm in diameter, peak of wavelength at 925 nm and angle of half sensitivity is 30 degree.

3.2 Optical sensor fixture design

The fixture is designed for holding all emitters and receivers so that four parallel projections beams' arrays can be created easily. For one optical sensor, the two orthogonal projections and two rectilinear projections are in the same layer. Practically, if all projections in one layer were to be made, three main problems will occur. First, Light from emitter must travel a longer distance to arrive receiver since the inner diameter of pipe used in system is already 85 mm. It means that the emitter itself must have a higher intensity capability. Unfortunately, for the emitter that has higher intensity, the physical size will be greater than 3 mm in diameter and also the cost will be come more expensive. Second, the developed fixture will look bulky. Third, since the radiant intensity of emitter is proportional to the forward current used, thus the power used for the whole system will increase. As a result, the fixture was constructed using two layers as shown in Figure 16. The upper layer is for two rectilinear projections and it contains 92 holes in total, 23 holes per side. The lower layer is for two orthogonal projections and it contains 64 holes in total, 16 holes per side. The distance between these two layers is 7 mm to prevent cracking in between both layers.

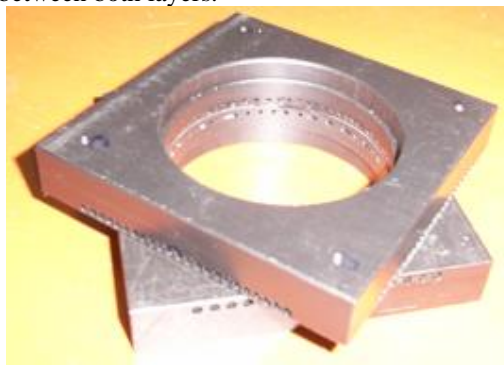


Figure 5. Fixture for holding emitters and receivers

The beam of light must diverge as little as possible to avoid overlapping of the received signals and lossness of the beam intensity [21]. Three methods are used to collimate the light source. First, uses infrared emitter and phototransistor that have small view angle. Second, places an optical stopper in front of the infrared emitter. In this system, ferrule is used as the stopper. This method is rather effective to limit the divergent angle [17]. The stopper is 1 mm in diameter and it successfully limits the light from the 3 mm infrared emitter as shown in Figure 17. Third, arrange all emitters and receivers in an alternate arrangement as shown in Figure 6. This arrangement helps to cut down the light divergent effect towards other sensors especially the receiver residing next to the designated receiver [17].

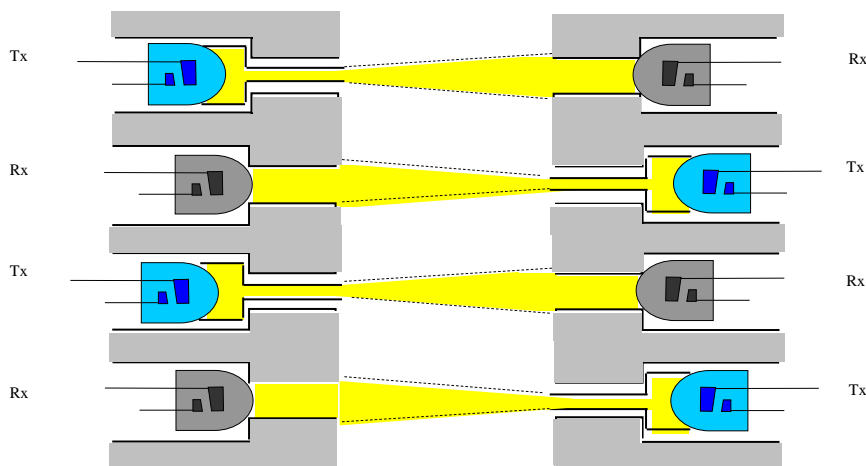


Figure 6. Optical stopper and alternate arrangement of sensors

3.3 Infrared projection circuit

In the system, a simple circuit is used and it connects the infrared emitter to a 100 ohm resistor with 5 volt supply. The circuit provides 50 mA to the emitter and it is good enough for the radiant intensity to project over 100 mm in distance. The circuit is shown in Figure 7.

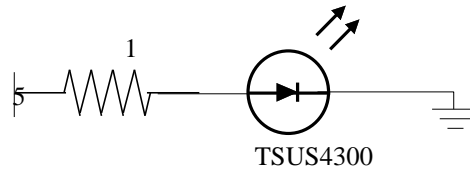


Figure 7. The emitter driver circuit

3.3 Signal conditioning circuit

The TEFT4300 phototransistor is a type of NPN transistor but no base connection available because the absorbed light plays the role of base current. The current created by the absorbed light is amplified by the bipolar action of the transistor, leading to a relatively large current flowing from collector to emitter. The phototransistor has higher sensitivity than the photodiode, so it produces more current for a given amount of incident light. Figure 8 shows the signal conditioning circuit that is specifically designed for this system. There are some factors that have to be considered when designing this circuit, such as the physical sizes of components, output voltage relative to light absorbed and components' cost. This circuit uses transistor instead of operational amplifier (op-amp) for signal amplification since the physical size of transistor is smaller and consists of 3 pins only. An important feature of the circuit is when no light is absorbed (object blocks the light), the output voltage produced is 5 volt; when light is absorbed (light not blocked), the output voltage produced is 0 volt. This feature can save the computation time in further processing of cross-correlation function in velocity measurement.

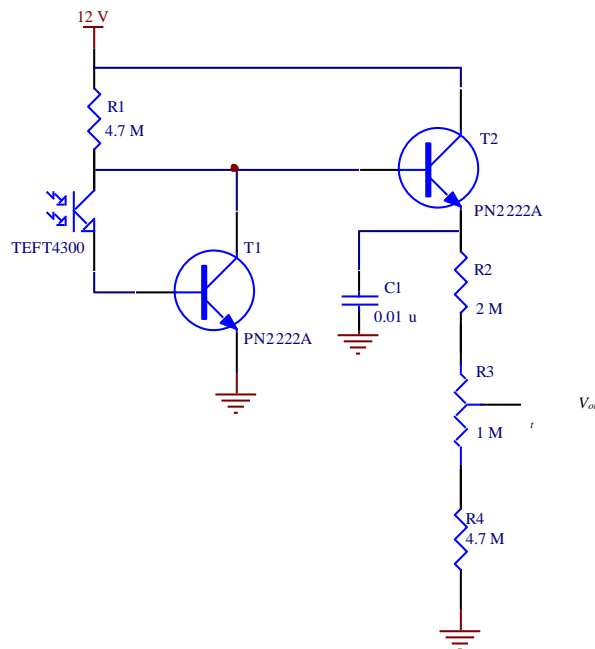


Figure 8. The signal conditioning circuit

To analyse the circuit, some equations are derived first as below,

$$I_{C(T1)} = I_{B(T1)} \times \beta \quad \dots 1$$

$$I_{B(T2)} = I_a - I_{C(T1)} \quad \dots 2$$

$$I_{E(T2)} = (1 + \beta) \times I_{B(T2)} \quad \dots 3$$

Substituting $I_{B(T2)}$ in equation 2 by using equations 1 and 2 resulting,

$$I_{E(T_2)} = (1 + \beta) \times (I_a - \beta I_{B(T_1)}) \quad \dots 4$$

where

- $I_{C(T_1)}$ = Collector current of transistor T₁
- $I_{B(T_1)}$ = Base current of transistor T₁
- β = DC current gain of transistor (also called h_{FE})
- $I_{B(T_2)}$ = Base current of transistor T₂
- I_a = Flow current as shown in Figure 19
- $I_{E(T_2)}$ = Emitter current of transistor T₂

In the case where projection light is not blocked, phototransistor will absorb all the light and $I_{B(T_2)}$ will equal to zero. From equation 3, $I_{E(T_2)}$ will be zero also and thus resulting $V_{out} = 0$ volt ideally. However, the light absorbed must be sufficient (in unblocked situation) to decrease $I_{B(T_2)}$ to zero. One of the factors that affect the light absorbed is the distance between emitter and phototransistor. If the distance is too long, the light absorbed will be less and causing $I_{B(T_2)}$ to be greater than 0 ampere. To solve this, an experiment is done to make sure V_{out} is approximately zero for the light absorbed after projecting 100 mm from source without any object blocking the light.

The light absorbed will decrease proportionally to the percentage of light being blocked by obstacle. Referring to equation 4, if the light absorbed decreases, $I_{B(T_1)}$ also decreases while output current of $I_{E(T_2)}$ increases. Since V_{out} is $I_{E(T_2)}$ multiplied with resistance used, V_{out} will be increased. The maximum output voltage can be produced if no light is absorbed by phototransistor. It is set to 5 volt so that the range of V_{out} is in between 0-5 volt. To set the maximum voltage, a voltage divider circuit is used and it is constructed by two fix resistors and one variable resistor. The calibration is carried out to tune the V_{out} to 5 volt in no blocking situation.

3.4 Sample and hold circuit

Sample and hold circuit can be defined as a device that acquires a signal and then stores it for a specified period of time before processing. It is recommended for optical tomography system because flow materials pass through sensor very fast resulting in more than a hundred varying sensors output voltage that need to be digitised. In addition, the circuit is useful to prevent data lost or wrong data captured per frame during instantaneous measurement.

3.5 Switching Circuit

As mentioned before, switching circuit is used to solve the limitation of data acquisition system. Referring to Figure 9, one analogue switch consists of an input, an output and a digital control logic. DG211CJ is the IC used in the circuit design. It contains four analogue switches in one chip. When digital control logic is '0', the switch is on. Inversely, the switch is off. The input of this circuit is connected to the output of sample and hold circuit.

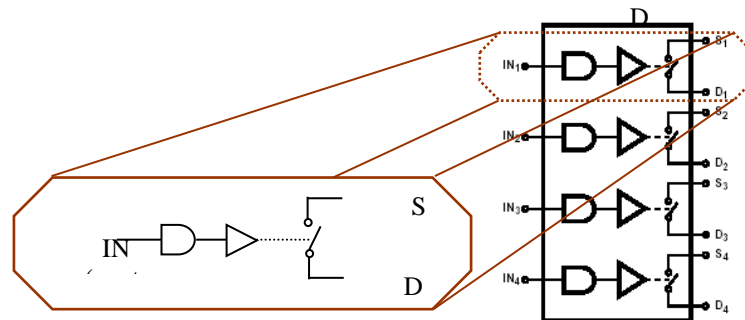
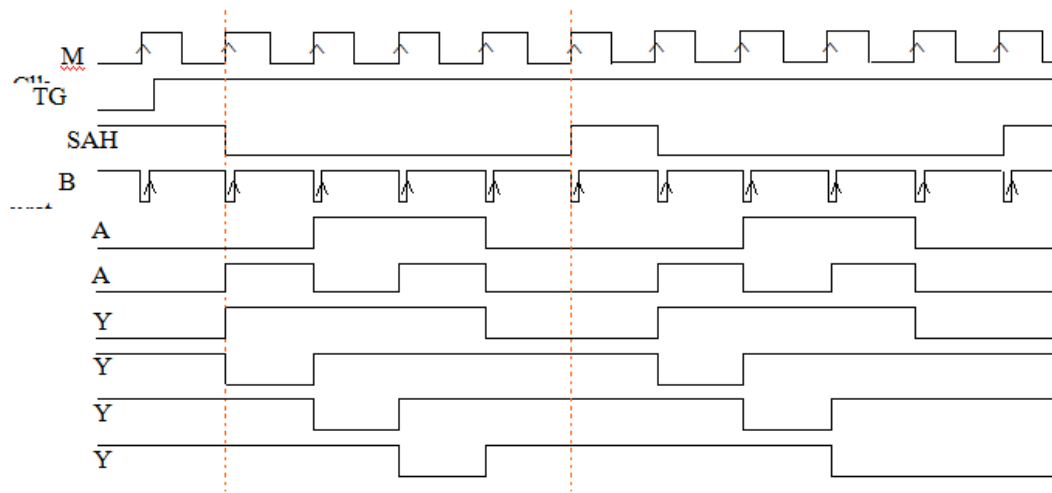


Figure 9. The DG211CJ analogue switch

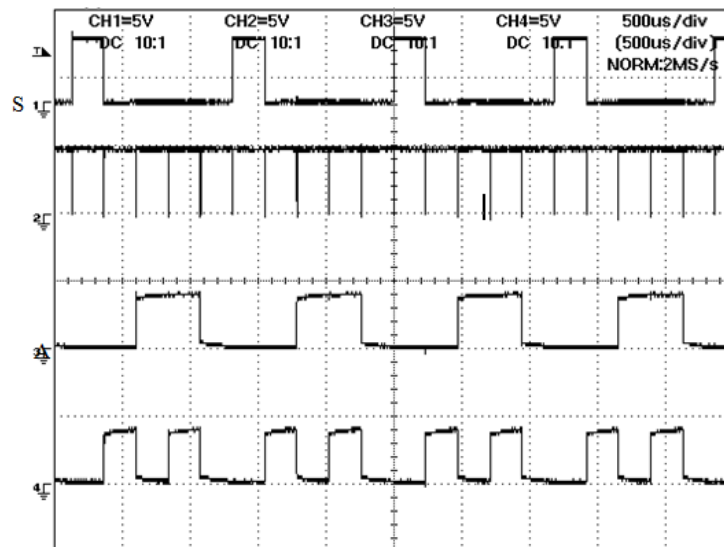
For each optical tomography sensor, it consists of a 16x16 layer and 23x23 layer. The 16x16 layer provides 32 output signals whereas the 23x23 layer provides 46 output signals. Therefore, one optical tomography sensor provides a total of 78 output signals that need to be digitised using the data acquisition system. In order to program the data acquisition system efficiently, the 78 output signals are digitised in two times, each time digitises 46 output signals. It means that for the first time, the data acquisition system digitises the output signals of 16x16 layer but only 32 signals are meaningful while remaining signals are useless. In the second time, the data acquisition system will digitise the output signals of 23x23 layer and all 46 signals represent sensor readings. Since this project consists of an upstream sensor and a downstream sensor, there are 4x46 signals that need to be digitised. The switching circuit of each layer has one logic control signal only. The control signal of 23x23 layer of upstream sensor is labelled Y_0 , control signal of 16x16 layer of upstream sensor is labelled Y_1 , control signal of 23x23 layer of downstream sensor is labelled Y_2 and control signal of 16x16 layer of downstream sensor is labelled Y_3 . These 4 control signals are generated from the digital signal control circuit.

3.6 Digital Signal Control Circuit

This circuit is very important in this project because a good design will result in high data capture rate. It is used to generate the digital signals as shown in Figure 10. For each signal, it's function is described in Table 2. The conversion process begins after the rising edge of TGOUT signal. It remains at 5 volt until the process finishes. The conversion process is dependant on how many set of data to be captured. The more set of data to be captured continuously, the longer of the conversion time is needed. The first rising edge of MClk after the triggering of TGOUT will set SAH signal to 0 volt to hold all output signals. After a small delay time of about 1.5 μ s (ensures signal $Y_0 - Y_3$ are in steady state), Burst signal will be in rising edge and this will trigger DAS to perform conversion of output signals of 16x16 layer of upstream sensor. Since the MClk signal has the frequency of 4.08 KHz, the 46 analogue signals will be completely converted in time of less than 243 μ s. The next three positive edge trigger of MClk will digitise the analogue signals from 23x23 layer of downstream sensor, 16x16 layer of downstream sensor and 23x23 layer of upstream sensor respectively. At the end of conversion of 184 analogue signals (1 set data), the SAH signal is triggered to resample all receivers' output voltages. In this cycle, although the burst signal triggers the DAS as usual but all 46 signals converted are useless and unrecorded in the software programmed. The following clock cycles of MClk signal repeat the previous process until all sets of data required are being captured.



(a) All digital timing and control signals needed



(b) Measured signals using oscilloscope

Figure 10. Digital timing and control signals for two optical tomography sensors

Table 2. Digital control signals function

Control signal	Function
MClk	Master clock to drive all other signals.
TGOUT	Trigger out signal from the data acquisition system. It will be in logic '1' when the data acquisition system is currently in operation.
SAH	Controls all sample and hold ICs.
Burst	As burst clock of DAS. It triggers the DAS to perform the conversion of 46 output signals.
A ₁ , A ₀	Both signals have the sequence 00, 01, 10, 11 to activate signals Y ₀ to Y ₃ .
Y ₀ - Y ₃	Control signals of switching circuit in 4 different layers.

To generate the MClk signal, a 555 timer is used to operate in the astable mode. The circuit connection is shown in Figure 11.

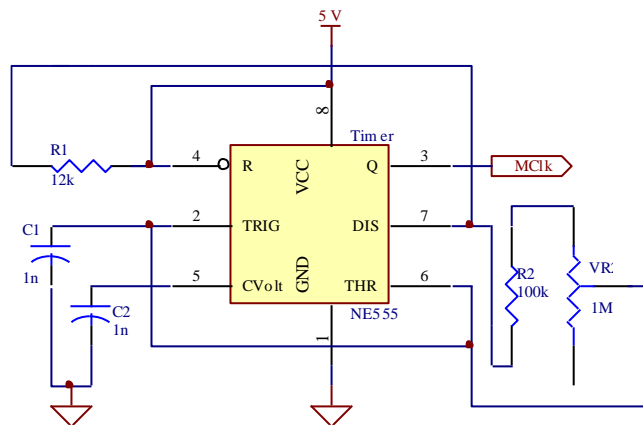


Figure 11. The 555 timer for generates MClk signal

To achieve the duty cycles of 50 percent, resistance of R₂+V_{R1} must be much greater than resistance R₁ so that the charging and discharging times of capacitor C₁ are approximately the same. The frequency of the signal is given by the following formula [18].

$$f_{MClk} = \frac{1.44}{(R_1 + 2(R_2 + V_{R1}))C_1} \quad \dots 5$$

Because of the frequency is 4.08KHz, R₁ is 12 KΩ, R₂ is 100 KΩ and C₁ is 1 nF, the trimmer V_{R1} must be tuned to 70.4 KΩ for obtains the signal desired. For the Burst signal, it is generated using retriggerable monostable multivibrator, 74HCT123 (refer to Figure 12). The logic '0' of the signal in each cycle is a small delay time to make sure control signals of the switching circuit, Y₀ – Y₃ are already in steady state before triggering the DAS for conversion. The delay time can be determined by calculating the pulse width based on the following equation,

$$t_w = 0.5 \times (R_{ext} + V_{R2}) \times C_{ext} \quad \dots 6$$

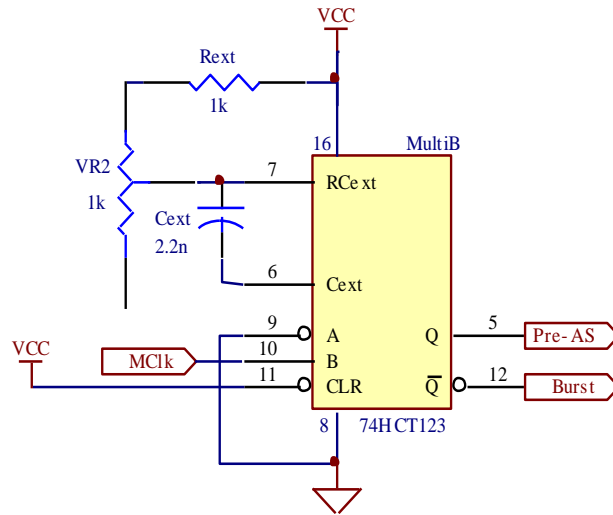


Figure 12. Circuit for generates Burst signal

The delay time that set to $1.5 \mu\text{s}$ is good enough to cover all transient respond of ICs, that is analogue switch takes $0.46 \mu\text{s}$ for turn on time and all other ICs in the HCT family that have propagation delay of nanoseconds each. Since C_{ext} is 2.2 nF and R_{ext} is $1 \text{ K}\Omega$, trimmer V_{R2} must be tuned to about 364Ω to achieve $t_w = 1.5 \mu\text{s}$.

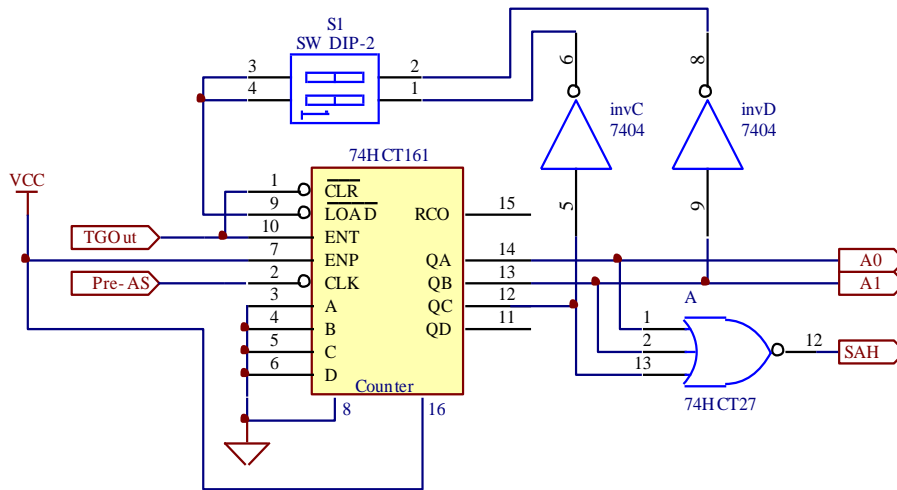


Figure 13. Circuit for generates A_0 , A_1 and SAH signals

Figure 13 shows the circuit to generate A_0 , A_1 and SAH signals. Note that one binary counter (74HCT161) and one DIP switch are employed. The DIP switch can select either the 2 sensors mode or 1 sensor mode that will be discussed later. The TGO ut signal from the DAS will control the pin enable and asynchronous master reset whereas the Pre-AS signal from the output of 74HCT123 will be the clock input to the counter. The output signals, A_0 and A_1 are connected to a 1-of-4 decoder (74HCT155) to generate the last 4 control signals, which are $Y_0 - Y_3$. There is also one DIP switch to select which mode to be used as shown in Figure 14.

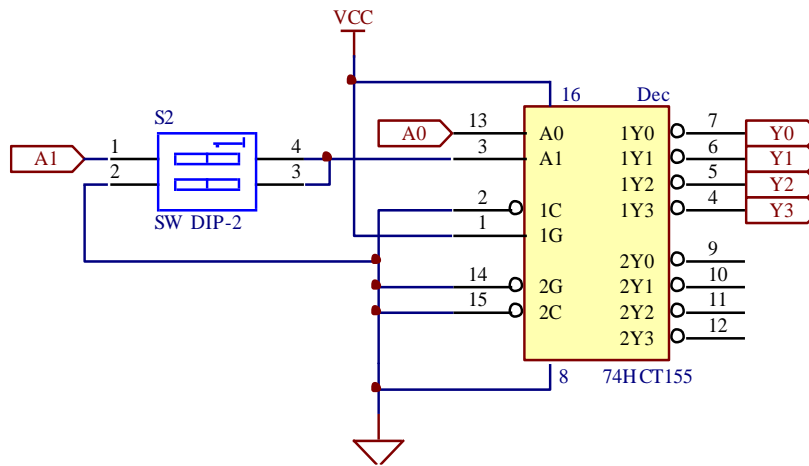
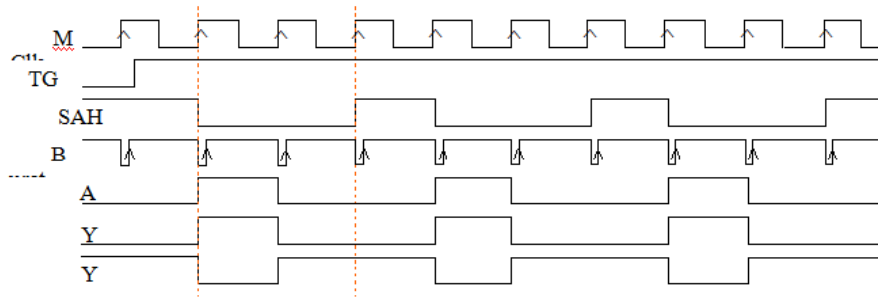
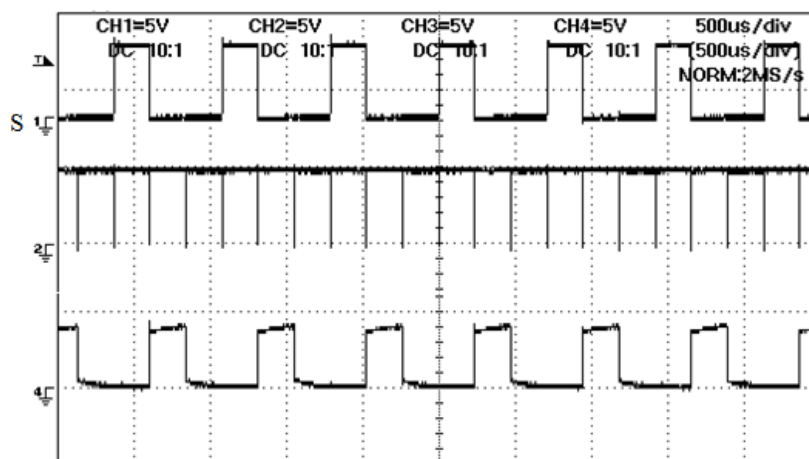


Figure 14. Circuit for generates $Y_0 - Y_3$ signals

For the hardware flexibility, the digital signal control circuit is designed in two modes. By selecting two sensors mode (switch 1 is on, switch 2 is off), all control signals generated are compatible with the 4 layers output signals conversion. If only one sensor is required in the measurement, the one sensor mode can be selected (switch 1 is off, switch 2 is on). This mode results in the control signals generated to be compatible with the conversion of two layers output signals. In this mode, the A_1 , Y_2 , and Y_3 signals are not needed; the remaining control signals are shown in Figure15.



(a) All digital timing and control signals needed



b) Measured signals using oscilloscope

Figure 15. Digital timing and control signals for one optical tomography sensor

4 RESULTS & DISCUSSIONS

The optical tomography sensor that successfully developed by using parallel beam projection technique is shown in Figure 16. The cross-sectional images inside the figure are reconstructed by using the sensor developed and Hybrid image reconstruction algorithm.

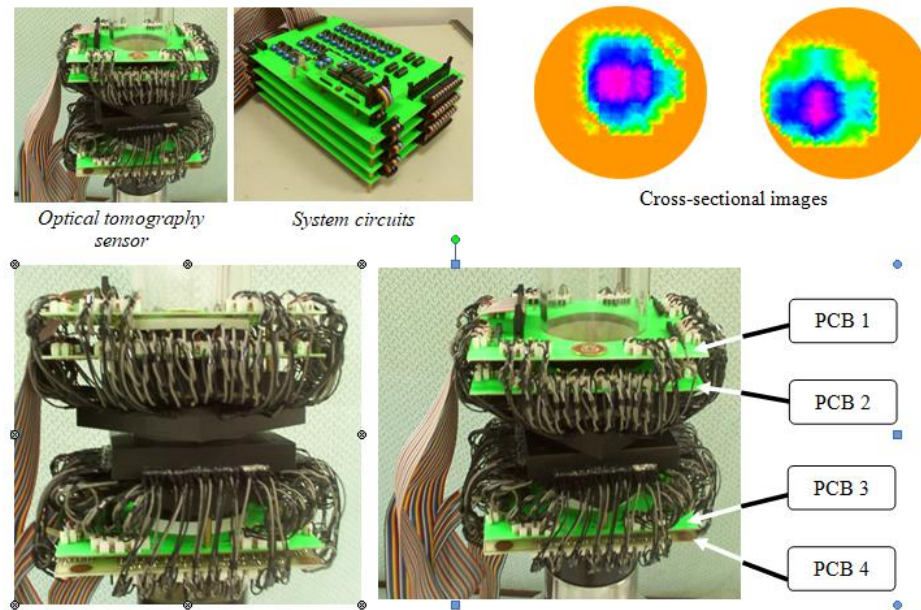


Figure 16. The developed optical tomography system

4.1 Real-time Image Reconstruction for Various Flow Regimes

There are 4 flow regimes created in this project referring to the research of Ruzairi [4]. They are full flow, three-quarter flow, half flow and quarter flow. Except the full flow regime, the other three regimes must create the corresponding baffle for blocking the necessary cross-sectional area as shown in Figure 17.

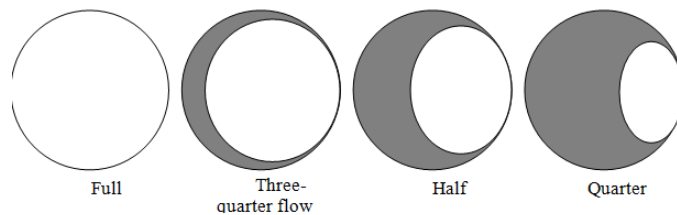


Figure 17. Baffle configurations for different flow regimes

In three quarter flow regime, the designed baffle cut-off three quarters area of pipeline so that clear for plastic beads flow. The three quarter flow expectation in pneumatic conveyor is illustrated in Figure 18(b). In half flow regime, the designed baffle cut-off half area of pipeline so that clear for plastic beads flow. The half flow expectation in pneumatic conveyor is shown in Figure 18(c). In quarter flow regime, the designed baffle cut-off quarter area of pipeline so that clear for plastic beads flow. The quarter flow expectation in pneumatic conveyor is illustrated in Figure 18(d).

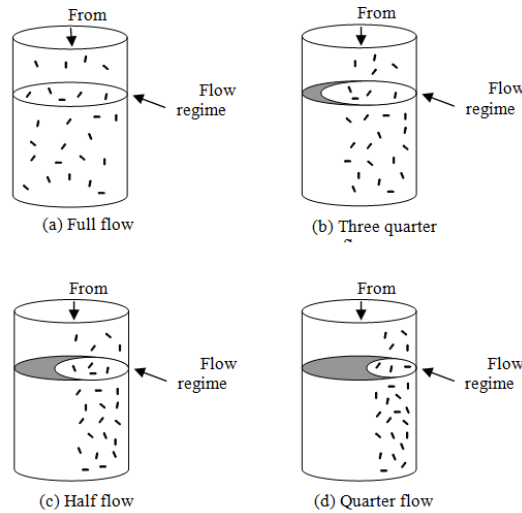


Figure 18. Flow expectation using regime of (a) full flow (b) three quarter flow (c) half flow (d) quarter flow

On the other hand, another kind of baffle is designed for fixing the mass flow rate of plastic beads. Three created baffle have the configuration as shown in Figure 19. The cut-off regions of these baffles are in the shape of circle with the diameter of 4.5 cm, 4 cm and 3.5 cm respectively. Based on the calibration results, these baffles can control and fix the specified mass flow rate in vertical flow rig as indicated in Figure 19.

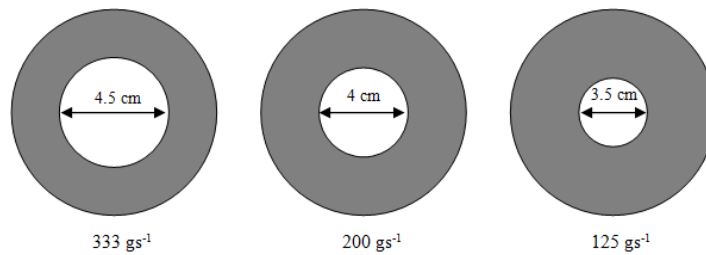


Figure 19. Baffle configurations for mass flow rate controlling

Referring to Figure 20, the vertical flow rig used for this section consists of a hopper, a valve, two gaps and optical tomography sensor. The valve operates as a switch to open and close the hopper to ensure that the plastic beads flowing inside the pipeline can drop down or be obstructed. Two gaps near to hopper are filled with the corresponding cut-off blade for controlling the mass flow rate and flow regime. The upper gap locates 3 cm below the valve and the lower gap locates 8 cm from the upper gap. The flow rate control baffle is inserted into upper gap whereas the flow regime baffle is inserted into lower gap. The pipeline of the flow rig has the inner diameter of 85 mm.

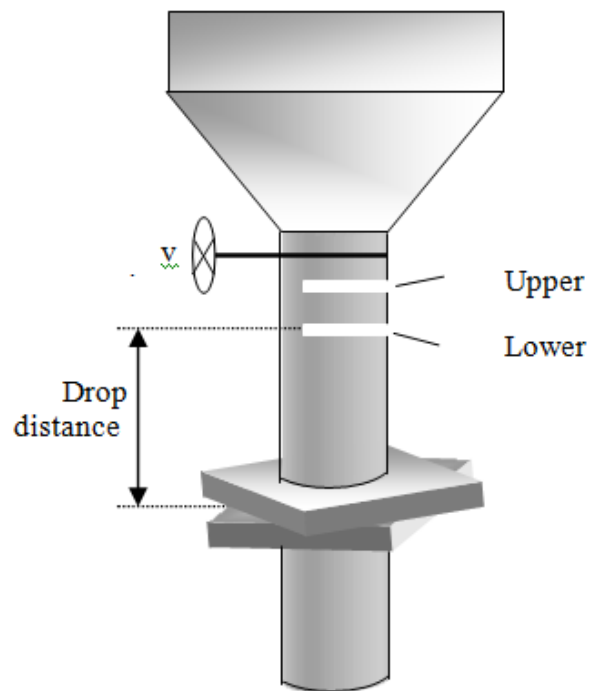
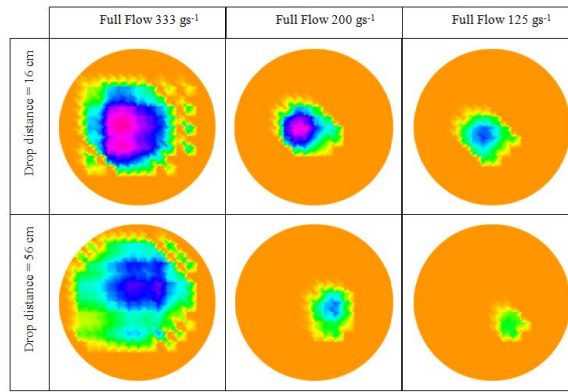
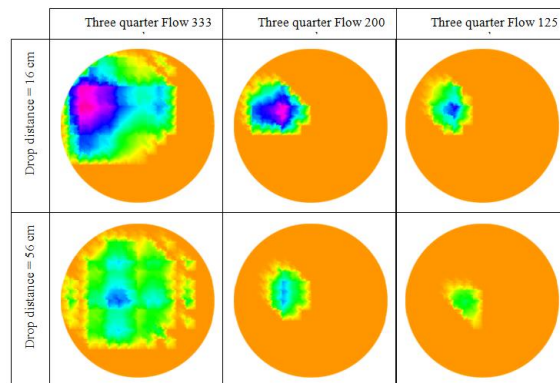


Figure 20. Vertical flow rig

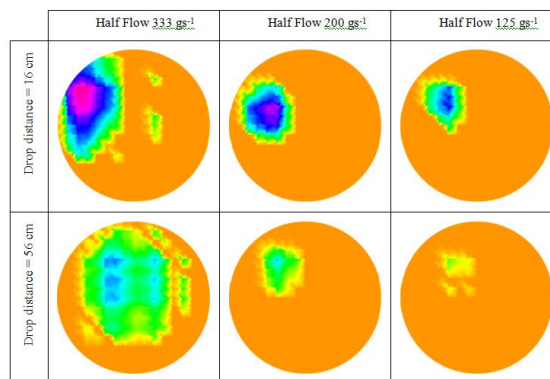
The measurement is carried out in the drop distance of 16 cm and 56 cm respectively. All of the cross-sectional images obtained are shown in Figure 21. These images can be realized by referring to a colour bar that showing the % ratio of light absorbed by the sensor (100% means the obstacle fully blocking the light transmitted)



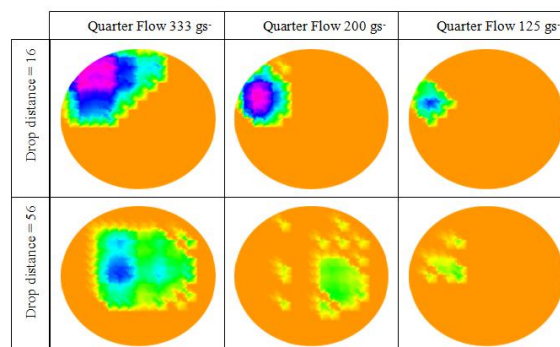
(a) Full flow regime



(b) Three quarter flow regime



(c) Half flow regime



(d) Quarter flow regime

Figure 21. Cross-sectional images for (a) Full flow regime (b) Three quarter flow regime (c) Half flow regime (d) Quarter flow regime

The results of this section are used to investigate the cross-sectional image reconstructed from two different drop distances. According to the images in Figure 33, it can be observed that the images with the drop distance of 16 cm have higher concentration compared to the drop distance of 56 cm. It is because the size of plastic bead is small and unable to block both 23x23 layer and 16x16 layer at the same time. For a short drop distance, the flow is heavy, dense and blocking both layers easily. When the flow passes through a long distance in gravity flow, it will be affected by velocity, wall friction and collision among the particles. These factors will make the flow of particles bounced, distributed within the pipeline and scattered. This can easily be proved by observing the half flow and quarter flow regimes in the flow rate of 333 gram/s, the cross-sectional image that constructed at the drop distance of 56 cm shows that the flow is distributed and unable to follow the given regime. Thus, the flow is unable to block both layers efficiently as the drop distance of 16 cm.

On the other hand, the images obtained from the drop distance of 16 cm shows that the flow follows the regimes but for the drop distance of 56 cm, most of the flow cannot follow the regimes. This case is mainly cause by the collision among the plastic beads. Since plastic bead itself has a strong elasticity, so the collision can make the plastic bead spring out from the origin flow. It will result problem in velocity measurement that based on the principal of cross-correlation flow measurement must in some patterns of material flow inside the conveyor travel without distortion between the upstream tomography sensor and downstream tomography sensor within an acceptable distance between the sensors (Beck and Plaskowski, 1987). However, the flow distribution will affect this measurement principal if the distance between upstream tomography sensor and downstream tomography sensor is long. It strongly believes that when using the flow materials such as dry sand, powder and sugar, this problem may not be so critical because their elasticity are weak. However, all results obtained show that the developed system has the capability to detect the concentration profile.

5 Conclusions

In conclusion, this paper has described the steps to construct an optical tomography system using two orthogonal and two rectilinear projections arrays. The success in the system development is surely beneficial to the further process measurement such as velocity and mass flow rate measurement.

REFERENCES

- [1] Xie, C.G. (1993a). "Electrical Capacitance Tomography (ECT)." *ECAPT 1993*. 225-228
- [2] Gladden, L.F. (1994) "Industrial Application of NMR Imaging", *Proc. ECAPT 1994*. Oporto, Portugal, March 24-26,1994. p466-477.
- [3] Williams, R.A. and Beck, M.S. (1995), Introduction To Process Tomography. in :- William, R.A. and Beck, M.S. (ed). *Process Tomography-Principle Techniques and Applications*. Great-Britain: Butterworth-Heinemann. 3-12.
- [4] Ruzairi Abdul Rahim (1996). *A Tomography Imaging System For Pneumatic Conveyors Using Optical Fibres*. Sheffield Hallam University. Ph.D. Thesis.
- [5] Froystein, T. (1993) "Gamma-ray Flow Imaging", *Proc. ECAPT 1993*. Karlsruhe, Germany, March 25-27,1993. p213-216
- [6] Jackson, R.G. (1995) "The development of optical systems for process imaging" in :- Williams, R.A. and Beck, M.S. (ed). *Process Tomography: Principles, Techniques and Applications*. Oxford : Butterworth-Heinemann Ltd, Chapter 10.
- [7] Xie, Z., Jackson, R. G., and Hartley, A. J. (1993) " Optical tomography of small bubble distribution measurement using filtered back projection algorithm" *Proc. ECAPT 1993*. Karlsruhe, Germany, March 25-27,1993. p174-177
- [8] Dugdale, W. P., Green, R.G., Hartley, A. J., Jackson, R.G. and Landauro, J. (1994b) " Characterization of single bubbles by an optical tomography system" *Proc. ECAPT 1994*. Oporto, Portugal, March 24-26, 1994. p81-92
- [9] Sallehuddin Ibrahim (2000). *Measurement Of Gas Bubbles In A Vertical Water Column Using optical Tomography*. Sheffield Hallam University. Ph.D. Thesis
- [10] Rzasz Mariusz R. and Dobrowolski, Boleslaw. (2000) "Evaluation of accuracy of reconstruction of air bubble shape in the computer-assisted of liquid aeration" *Proc. 1st International Symposium On Process Tomography*. Jurata

- [11] Chan Kok San (2002). *Real Time Image Reconstruction For Fan Beam Optical Tomography System.* " Universiti Teknologi Malaysia. M.Sc. Thesis
- [12] Lucas, N., Jackson, R.G., Hartley, A. J., and Spooner, R. C. (1994) "Optical tomography for combustion monitoring in an Engine" *Proc. ECAPT 1994*, Oporto, Portugal, March 24-26,1994. p42-49
- [13] Daniels, A. R., Basarab, I., Dickin, F. and Green, R. G. (1993) " Initial developments of an optical matrix imaging system for sewers" *Proc. ECAPT 1993*. Karlsruhe, Germany, March 25-27,1993. p05-108.
- [14] Dugdale, W. P. (1994a) "An optical instrumentation system for the imaging of two-component flow" University of Manchester : Ph.D. Thesis
- [15] Ruzairi Abdul Rahim , Pang Jon Fea, Chan Kok San and Leong Lai Chen (2005), "Area of Concentration Measurement Using Optical Tomography Technique for Various Flow Patterns", *Jurnal Teknologi*, Jun 2005, UTM Publisher
- [16] R.Abdul Rahim, K.S.Chan "Optical Tomography System for Process Measurement Using LED as a Light Source", *Journal Optical Engineering*, Volume 43, Issue 5, pp. 1251-1257, May 2004
- [17] R.Abdul Rahim, K.S.Chan , "Application of optical Tomography in Real Time monitoring for Solid Particles", *Jurnal ElektriKa*, December 2004, Pp 28, vol 6
- [18] Floyd, T.L. (1999). "*Electronic Devices.*" 5th ed. Upper Saddle River, N.J.: Prentice-Hall